[22]

A. DI GERLANDO - I. VISTOLI

D.C. POLARIZED CURRENT TRANSFORMERS FOR THE MEASUREMENT OF HARMONIC NOISE: DESIGN AND MODELLING METHODOLOGIES

ICHPS V - INTERNATIONAL CONFERENCE
ON HARMONICS IN POWER SYSTEMS

ATLANTA (GA USA), 22-25 SETTEMBRE 1992

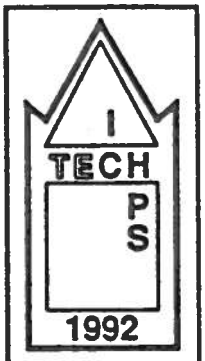

ICHPS V

International Conference on Harmonics in Power Systems

September 22-25, 1992

Swissôtel
Atlanta, GA USA

Sponsored by:
IEEE Power Engineering Society

D.C. POLARIZED CURRENT TRANSFORMERS FOR THE MEASUREMENT OF HARMONIC NOISE: DESIGN AND MODELLING METHODOLOGIES

Antonino Di Gerlando Ivo Vistoli

Dipartimento di Elettrotecnica, Politecnico di Milano
Piazza Leonardo da Vinci, 32 - 20133 Milano, Italy

Abstract - The paper describes an algorithm for the design of a special current transformer (C.T.), suited to measure the residual harmonic content of fluctuating direct currents, generated by static convertors on their D.C. side. An in-depth study of a C.T. model has been carried out in order to analyse the entire frequency band covered by the device.

INTRODUCTION

In many D.C. equipments, connected to A.C. installations via static convertors, the measurement of the residual level of harmonics generated on the D.C. side of the convertors is a problem of considerable importance. It is sometimes necessary to estimate A.C. components of a substantially lower amplitude than that of the direct current, over a frequency band ranging from some Hz to several kHz.

The situation of D.C. traction installations is typical of this field: for example, some specifications [1] about on board convertors place limits for the A.C. components of the order of $10^{-3} \div 10^{-4}$ times the D.C. component, from some Hz to 10 kHz.

In the absence of suitable filtering, the existence of the D.C. component at the transducer output creates various problems, in particular for the harmonic analyser: the accuracy and resolution of the latter are related to the maximum instantaneous value of the signal to be analysed, and hence is strongly affected by the presence of the D.C. component.

The use of a suitably proportioned C.T., as an interface between the power circuit and the measurement circuit, gives a number of advantages, such as the galvanic insulation and the filtering of the D.C. component (without employing high-pass filters).

The design of the C.T. is affected by the high value of the D.C. component, which necessitates the adoption of a gapped magnetic core; on the other hand, the presence of the air-gap implies high values of magnetizing current for the A.C. components.

Apart from winding data and core dimensions, the highest ratio errors are found at low frequencies, where the primary current is mainly magnetizing, and at high frequencies, where the secondary leakage reactance increases and capacitive-type phenomena appear.

C.T. DESIGN

The design procedure must satisfy the following conditions:
- low ratio error;
- low influence of amplitude, of both the D.C. and A.C. components, on the ratio error (this means that the C.T. must have a good linearity, which makes it possible to refer to a single error/frequency calibration curve, practically independent of the input signal amplitude);
- limited mass of magnetic material and copper, for reasons of space and cost;
- adequate amplitude of the voltage V_m across the measuring resistance R_m; in many cases, this permits a direct connection to the spectrum analyser, without the need for a signal amplifier.

The method of designing the gapped C.T. is based on the approximate model of such a transformer, which is valid when working at a low frequency [1]: when compared with the complete "T" circuit model of the C.T., the approximation consists of ignoring:
- the secondary leakage inductance ($L_2 \approx 0$);
- the conductance of the derived branch ($G_0 \approx 0$).

The structure adopted for the magnetic core of the C.T. is the "double C". This uses two gaps of width δ and consists of alloy laminations with a thickness not exceeding 0.3 mm. In what follows, however, reference will be made to a toroidal-type magnetic core, equivalent to the "double C" type adopted, that is having the same net cross-section A_n and the same average length ℓ_n. This does not alter the results and permits simpler expressions for the quantities of interest [1].

The toroidal core is defined by its internal diameter D_n and by the radial and axial dimensions (a_n and b_n respectively) of the core section.

As for the magnetic material, the presence of a powerful D.C. magnetization, with a low-amplitude A.C. component superimposed, leads to the use of the reversible permeability (μ_{rev}) instead of the normal one (μ). The reversible permeability μ_{rev} can be evaluated as follows [2]:

$$\mu_{rev} \approx \mu_i \cdot \left(1 - \frac{B_{dc}}{B_{sat}}\right)^k \quad , \qquad (1)$$

where:
μ_i is the initial permeability of the normal magnetization curve; B_{sat} is the saturation flux density of the magnetic material; k is an exponent which depends on the type of material ($k = 0.75 \div 2$); B_{dc} is the D.C. polarization flux density.
While the first three parameters represent physical characteristics intrinsic of the magnetic material adopted, the choice of the value of B_{dc} constitutes a degree of freedom in the design.

A review of commercial materials available suggests the adoption of a Mumetal core ($\mu_i \approx 25 \cdot 10^3 \cdot \mu_0$; $B_{sat} \approx 0.7$ T; $k \approx 0.75$).

The calculation algorithm

The basic specification quantities needed to define the design (defined according to a predetermined minimum reference angular frequency: $\tilde{\omega}$) are:
- amplitude of the D.C. component of primary current: I_{dc};
- amplitude of the A.C. component of primary current: I_1;
- amplitude of the voltage across the measuring resistance R_m: V_m.

The design parameters are as follows:
- ratio error ($\varepsilon = 1 - I_2/I_{1s}$, with $I_{1s} = I_1 \cdot N_1/N_2$) at the reference angular frequency $\tilde{\omega}$: $\tilde{\varepsilon}(\tilde{\omega})$;
- magnetic material characteristics: B_{sat}, μ_i, k;
- current density of the D.C. primary component: S_{dc};
- fill factors (α_{f1}, α_{f2}) of the primary and secondary windings;

- lamination packing factor: K_{st};
- ratio between the dimensions of the core cross-section: $K_L = b_n/a_n$;
- core coefficient, equal to the ratio between radial width and diameter: $K_n = a_n/D_n$;
- ratio between gap width and diameter: $K_g = \delta/D_n$;
- number of primary turns: N_1.

The calculation proceeds on the basis of the design specifications and parameters, as described below. For greater clarity, the formulae comprising the design algorithm are boxed.

The reversible permeability is evaluated from eq.(1), having assumed for B_{dc} a value sufficiently lower than the saturation level:

$$\mu_{rev} \approx \mu_i \cdot \left(1 - \frac{B_{dc}}{B_{sat}}\right)^k \quad . \qquad (1)$$

The core magnetic factor λ_n (equal to the ratio between the magnetic half-length of the core and the geometrical gap: $\lambda_n = [(\ell_n/2)/(\mu_{rev}/\mu_o)]/\delta$, see [1]) is calculated using the following expression:

$$\lambda_n = \frac{\pi \cdot (1 + K_n)}{2 \cdot (\mu_{rev}/\mu_o) \cdot K_g} \quad . \qquad (2)$$

Starting from the dimensioning formula (see [1]):

$$N_2 \cdot D_n^2 = \frac{1 + \lambda_n}{\sqrt{2 \cdot \tilde{\varepsilon} - \tilde{\varepsilon}^2}} \cdot \frac{1}{\tilde{\omega}} \cdot \frac{1}{K_{st} \cdot K_L \cdot K_n^2} \cdot \frac{V_m}{B_{dc}} \cdot \frac{I_{dc}}{I_1} \quad , \qquad (3)$$

and putting χ equal to:

$$\chi = \frac{(1 + \lambda_n) \cdot V_m}{\sqrt{2 \cdot \tilde{\varepsilon} - \tilde{\varepsilon}^2} \cdot \tilde{\omega} \cdot K_{st} \cdot K_L \cdot K_n^2} \quad , \qquad (4)$$

we can write:

$$N_2 = \frac{\chi \cdot I_{dc}}{B_{dc} \cdot I_1 \cdot D_n^2} \quad ; \qquad (5)$$

finally, putting $D_n = \delta/K_g$ in eq.(5) and substituting for parameter δ the expression obtainable from the following equation:

$$B_{dc} \simeq \mu_o \cdot N_1 \cdot I_{dc}/(2 \cdot \delta) \quad , \qquad (6)$$

we obtain:

$$N_2 = \frac{4 \cdot \chi \cdot K_g^2 \cdot B_{dc}}{\mu_o^2 \cdot N_1^2 \cdot I_{dc} \cdot I_1} \quad ; \qquad (7)$$

this equation can be effectively used to calculate the number of secondary turns N_2 because, unlike eqs.(3) and (5), it contains specification values and design parameters.

It is now possible to obtain the following geometrical parameters from eq.(5):

$$D_n = \sqrt{\frac{\chi \cdot I_{dc}}{N_2 \cdot B_{dc} \cdot I_1}} \quad , \qquad (8)$$

$$a_n = K_n \cdot D_n, \qquad b_n = K_L \cdot a_n, \qquad \delta = K_g \cdot D_n \quad . \qquad (9)$$

Bearing in mind that the A.C. component I_1 has an RMS value much lower than the D.C. component I_{dc}, the cross-section (A_{c1}) of the primary winding conductor and the corresponding net (A_{r1}) and gross (A_{i1}) winding cross-sectional areas can be calculated thus:

$$A_{c1} = I_{dc}/S_{dc}, \quad A_{r1} = N_1 \cdot A_{c1}, \quad A_{i1} = A_{r1}/\alpha_{r1} \quad . \qquad (10)$$

With regard to the secondary winding, if the area of the core window is denoted A_w, we have:

$$A_w = \frac{\pi}{4} \cdot D_n^2, \quad A_{i2} = A_w - A_{i1}, \quad A_{r2} \leq \alpha_{r2} \cdot A_{i2}, \quad A_{c2} = \frac{A_{r2}}{N_2} \quad ; \qquad (11)$$

as can be seen from eq.(11), the maximum cross-section of the secondary winding conductor is determined only by the amount of space available in the window, as the value of the secondary current is very low.

The average length of a secondary winding turn (wound directly around the core) can be estimated from the following equation:

$$\ell_{m2} \approx \left[2 \cdot K_n \cdot (1 + K_L) + \xi_{i2}\right] \cdot D_n \quad , \qquad (12)$$

having put: $\xi_{i2} = A_{i2}/A_w$.

The resistance of the secondary winding is given by:

$$R_2 = \rho \cdot \ell_{m2} \cdot N_2/A_{c2} \quad , \qquad (13)$$

while the (theoretical) value of the measuring resistance is:

$$R_m = \frac{V_m}{(N_1/N_2) \cdot I_1 \cdot (1 - \tilde{\varepsilon})} \quad . \qquad (14)$$

Finally, the masses of the ferromagnetic core (M_n) and the copper of the secondary winding (M_{r2}) are given by:

$$M_n = \gamma_n \cdot K_n^2 \cdot (1 + K_n) \cdot K_L \cdot \pi \cdot D_n^3, \quad M_{r2} = \gamma_r \cdot N_2 \cdot \ell_{m2} \cdot A_{c2} \quad , \qquad (15)$$

where γ_n and γ_r are the densities of the ferromagnetic material and copper respectively.

The prototype constructed

Using the procedure described above, a prototype of a C.T. with an air-gap has been designed and constructed with the characteristics as shown in the Table.

Nominal and specification data	
direct current primary component:	I_{dc} = 20 A
alternative current primary component:	I_1 = 40 mA RMS
voltage at the terminals of R_m:	V_m = 250 mV RMS
reference frequency:	$\tilde{f}$ = 10 Hz
reference current ratio error:	$\tilde{\varepsilon}$ = 5 %
Characteristics of the prototype	
magnetic material: Mumetal, lam. thickness:	0.3 mm
equivalent internal core diameter:	D_n = 75 mm
radial core width:	a_n = 55 mm
axial core lenght:	b_n = 50 mm
air gap thickness:	δ = 0.16 mm
number of primary turns:	N_1 = 5
number of secondary turns:	N_2 = 8000
resistance of the secondary winding:	R_2 =700 Ω
measurement resistance:	R_m = 10 kΩ
primary conductor: 2 wires, diameter:	d_{c1} = 2 mm
secondary conductor: 1 wire, diam.:	d_{c2} = 0.25 mm

The transformer employs a "double C" type core and the windings are distributed on each half of the core. In order to reduce the leakage flux, the secondary is wound directly around the core; as the primary winding is physically connected to a power circuit, it is insulated and suitably spaced away from the secondary.

The values in the Table make it clear that, in this type of C.T., the secondary winding operates in a condition far removed from a short-circuit. In reality, both the internal resistance of the secondary winding and, above all, the measuring resistance have unusually high values.

It should also be noted that:
- referring to the value of I_1 in the Table and considering the turn ratio, the secondary currents are of the order of some μA;
- an approximate evaluation of the A.C. component of core flux density gives values of some μT at low frequency, which reduce to a few nT at higher working frequencies.

These very low values of electrical and magnetic quantities impose the necessity of sufficient screening of the device by means of a suitable metallic container, so as to make it safe from the effects of radiated electromagnetic disturbances.

Sensitivity of design parameters at low frequencies

In examining this aspect, the following assumptions have been made:
- reference has been made to the design algorithm described above: only the input quantities are the variables having a direct influence on the design, the variation of which is being studied. It is hence clear that the parameter sensitivity also depends on the structure of the adopted algorithm and that it can vary, even substantially, in the case of a different design method;
- given the large number of variables involved, it has been judged useful to apply variation only to the more important ones, taken one at a time. This approach method clearly does not allow us to find the optimum design condition of the device, but it has the advantage of permitting a rapid display of parametric sensitivity;
- all the quantities at the design output are expressed in p.u. and referred to corresponding values of the C.T. described in the Table and they are marked with a dot at the top;
- the graphs only show the behaviour of the quantities which vary as a function of the parameter being considered, meaning that the remaining ones coincide with those of the reference C.T..

a) Ratio error at the reference frequency: $\tilde{\varepsilon}$.

Fig.1 shows that, as the permitted ratio error increases, the number of secondary turns ($\dot{N}z$) decreases and the dimensions and mass ($\dot{M}n$) of the core and the air-gap (δ) remain unchanged. At the same time, the secondary resistance ($\dot{R}z$) and the measuring resistance ($\dot{R}m$) decrease, while the diameter ($\dot{d}cz$) of the secondary wire increases. The mass of the secondary winding ($\dot{M}rz$) and the core magnetic factor ($\dot{\lambda}n$) do not change.

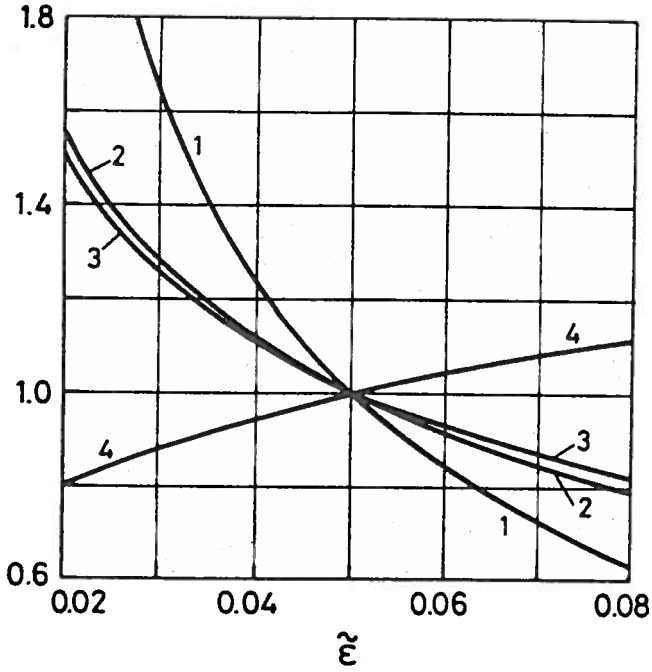

Fig.1. Sensitivity of the design parameters to $\tilde{\varepsilon}$: 1=$\dot{R}z$; 2=$\dot{N}z$; 3=$\dot{R}m$; 4=$\dot{d}cz$.

These results might lead, paradoxally, to the conclusion that the choice of different values of the ratio error results in C.T.s all having the same dimensions and weights. In practice, one cannot adopt values of ratio error which are too low, because this implies an excessive number of secondary turns, with values of wire diameter which are too low. Apart from causing difficulties in construction, this can lead to unacceptable performance at high frequencies because of increased effects of capacitance.

On other hand, eq.(3) leads to the conclusion that, if, as $\tilde{\varepsilon}$ increases, the number of turns $\dot{N}z$ is kept constant instead of assuming unchanged the diameter $\dot{D}n$, the latter assumes a decreasing value, hence a reduction in the size and the mass of the C.T..

Finally, it must be noted that excessively high values of the measuring resistance $\dot{R}m$ cause serious problems with regard to instruments connected across the measuring terminals. In order to ensure that the instrument does not affect the functioning of the transducer, the instrument itself should have a sufficiently high input impedance, much higher than the resistance $\dot{R}m$.

b) Ratio between air-gap (δ) *and diameter* ($\dot{D}n$) *of the core*: K_g.

This ratio cannot be allowed to vary within wide limits, particularly towards lower values, because of technological limits in the construction of accurate values of small gap widths. Fig.2 shows the effect of variation in the parameter K_g. In the calculations, the same value of the air-gap, equal to that of the reference C.T., has been maintained.

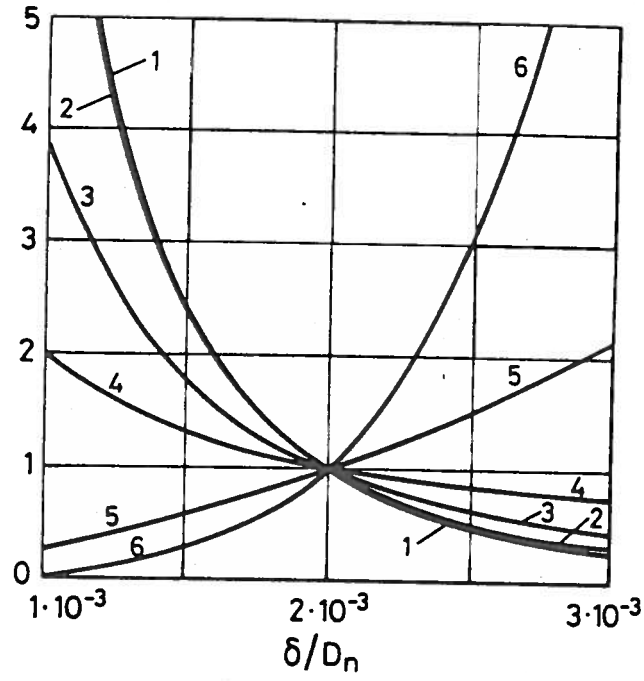

Fig.2. Sensitivity of the design parameters to $\delta/\dot{D}n$: 1=$\dot{M}rz$; 2=$\dot{M}n$; 3=$\dot{d}cz$; 4=$\dot{D}n$=$\dot{a}n$=$\dot{b}n$=$\dot{\lambda}n$; 5=$\dot{N}z$=$\dot{R}m$; 6=$\dot{R}z$.

When the parameter K_g grows, the following happens:
- the core diameter ($\dot{D}n$) and the other dimensions ($\dot{a}n$) and ($\dot{b}n$) decrease;
- the mass of the core ($\dot{M}n$) and of the secondary winding copper ($\dot{M}rz$) as well as the secondary wire diameter ($\dot{d}cz$) decrease;
- similarly, the number of secondary turns ($\dot{N}z$) and the measuring resistance ($\dot{R}m$) increase, while the secondary resistance ($\dot{R}z$) increases very rapidly.

Summarising, a reduction in diameter at a constant air-gap leads to a more favourable design of the C.T. as far as mass is concerned. The reduction in the core magnetic factor ($\dot{\lambda}n$) is also a favourable feature, insofar as it reduces the sensitivity of the transducer to amplitude variations in the D.C. and A.C. components. However, such a reduction in dimensions requires an increase in the number of secondary turns, which can produce problems, already described.

c) Core coefficient: $K_n = a_n/\dot{D}n$.

This variation is carried out at constant diameter.

An increase in K_n (fig.3) leads to an increase in the external dimensions of the core, which becomes increasingly heavier. The mass of the secondary copper increases in the same proportion and there is a slight increase in the core magnetic factor λ_n.

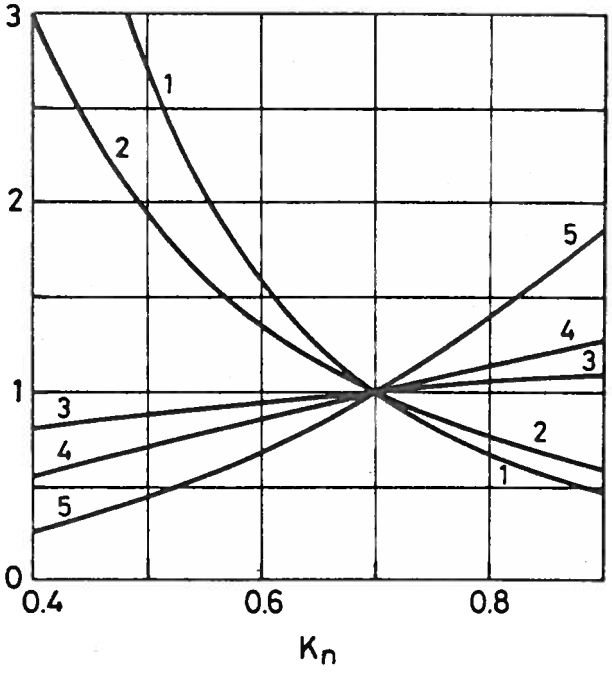

Fig.3. Sensitivity of the design parameters to K_n: 1=R_z; 2=N_z=R_m; 3=λ_n; 4=d_{cz}=M_{rz}=a_n=b_n; 5=M_n.

Against these negative aspects, there are the advantages of a substantial reduction in the number of secondary turns, as well as in the R_z and R_m resistances.

d) Number of primary turns: N1.

As the number of primary turns increases (see fig.4), the air-gap (δ) increases linearly with it, together with the core dimensions (D_n, a_n, b_n).

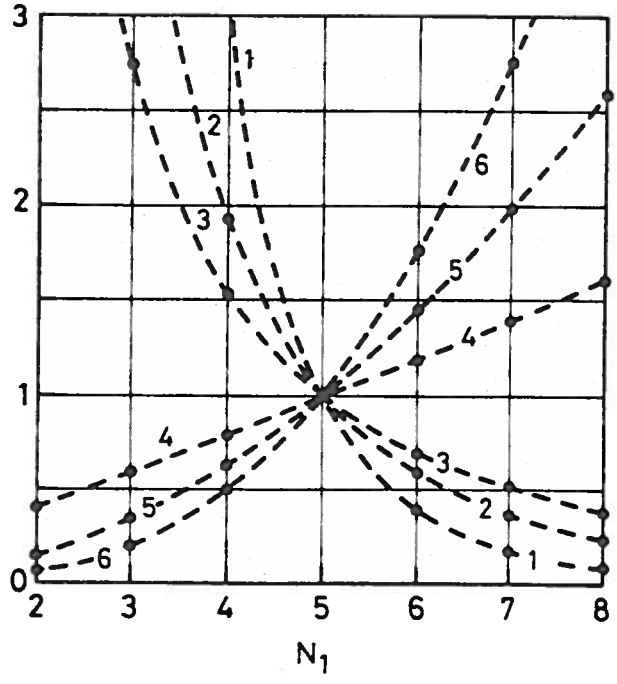

Fig.4. Sensitivity of the design parameters to N_1: 1=R_z; 2=R_m; 3=N_z; 4=δ=D_n=a_n=b_n; 5=d_{cz}; 6=M_{rz}=M_n.

The masses of the core and of the secondary copper (M_n, M_{rz}) and the diameter of the secondary wire (d_{cz}) increase rapidly, while the number of secondary turns N_z and the resistances R_m and R_z decrease.

e) Initial relative permeability: μ_i/μ_o.

The variation in this parameter corresponds to the choice of various types of magnetic material. This variation applies at constant core dimensions and at a constant mass of the secondary copper (fig.5).

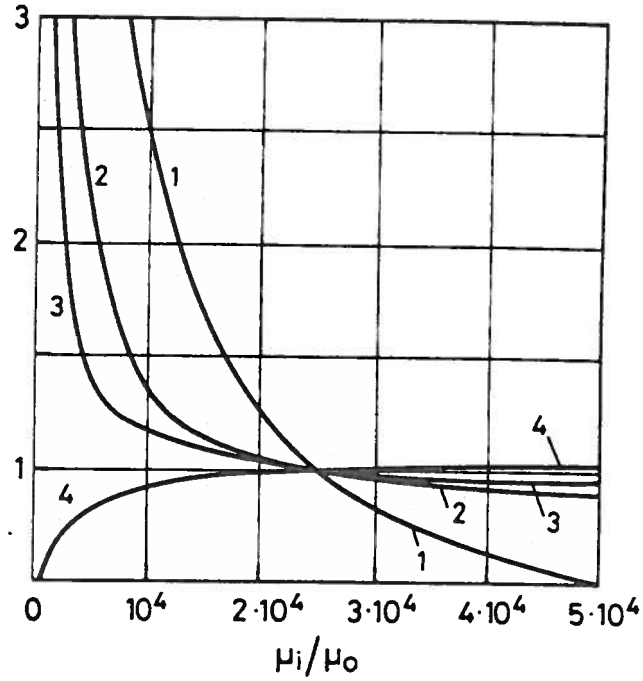

Fig.5. Sensitivity of the design parameters to μ_i/μ_o: 1=λ_n; 2=R_z; 3=N_z=R_m; 4=d_{cz}.

It can be seen that, as μ_i/μ_o increases, this leads to a reduction in the number of secondary and measuring resistances.

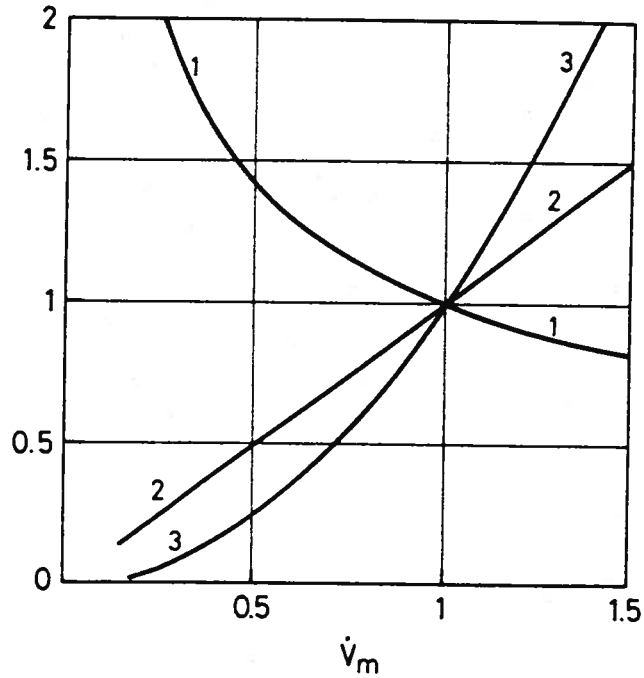

Fig.6. Sensitivity of the design parameters to $\dot{V}_m$: 1=d_{cz}; 2=N_z; 3=R_z=R_m.

At the same time, an increase in the diameter of the secondary wire is noted. These variations, which are considerable in the region where the ratio μ_i/μ_o is low (corresponding to the use of lower-quality magnetic materials), become much smaller in the region of high initial permeability.

The only parameter which shows a substantial reduction when the initial permeability increases is the core magnetic factor λ_n. Bearing in mind that high values of this factor are associated with a high sensitivity of the C.T. to variations in the amplitudes of the D.C. (I_{dc}) and A.C. (I_1) components of the primary current, the advantage of using magnetic materials with a high initial permeability μ_i becomes clear.

f) Voltage across the measuring resistor: V_m

The core dimensions and the width of the air-gap are kept constant, thus the masses of the core and of the secondary copper also remain constant (fig.6).
As the measuring voltage V_m increases, the number of secondary turns (N_2) increases linearly with it, while the secondary and measuring resistances (R_2, R_m) increase rapidly. At the same time, the diameter of the secondary wire decreases.

Other considerations stated under point *a)* above could also be repeated here.
It can be concluded that a low value of voltage V_m is associated with a more favourable transducer design. However, very low values of V_m require the use of an amplifier stage.

SIMULATION MODEL FOR THE STUDY OF CAUSES OF C.T. ERRORS

The only cause of error considered when working at low frequencies was the magnetizing current. The study of the C.T. over the entire working frequency range requires the use of more complete models. It is therefore necessary to examine the mechanism and significance of the following phenomena:
- behaviour of ferromagnetic materials at high frequencies;
- leakage fluxes;
- effects of resonance and attenuation caused by parasitic capacitances.

Ferromagnetic materials in high frequency operation

As is well known, magnetic materials subjected to alternating fields exhibit two types of loss: hysteresis and eddy currents losses.
The specific condition in which the material finds itself in the present application (small alternating component superimposed on a large D.C. component) makes it difficult to evaluate hysteresis losses, associated with highly asymmetrical magnetization cycles. On the other hand, the higher the frequency, the greater is the relative significance of eddy losses as compared with hysteresis losses. Because of this, in the following only the effects of eddy currents are considered.

The use of the classic concept of complex reluctance [3] is one of the ways of simultaneously keeping track of magnetizing and dissipative effects of eddy currents. Denoting with θ_o the D.C. reluctance operator (equal to the ratio between the magnetic drop voltage U and the resulting flux Φ in a generic branch of the magnetic circuit), in the sinusoidal operation, the operator which links the phasors of magnetic voltage $\bar{U}$ and the flux $\bar{\Phi}$ is a complex quantity, expressed as follows:

$$\bar{\theta} = \frac{\bar{U}}{\bar{\Phi}} = \theta_o \cdot K_\theta(\xi) \cdot \left[1 + j \cdot \alpha(\xi)\right] \quad , \qquad (16)$$

where:

$$K_\theta(\xi) = \xi \cdot \frac{\sinh(2\cdot\xi) + \sin(2\cdot\xi)}{\cosh(2\cdot\xi) - \cos(2\cdot\xi)} \quad ,$$

$$\alpha(\xi) = \frac{\sinh(2\cdot\xi) - \sin(2\cdot\xi)}{\sinh(2\cdot\xi) + \sin(2\cdot\xi)} \quad ,$$

with $\xi = \frac{s/2}{s_p}$, $s_p = \sqrt{\frac{\rho}{\pi \cdot f \cdot \mu_{rev}}}$;

s is the lamination thickness and s_p is the penetration depth.
It can be seen that, at low frequency, the complex reluctance $\bar{\theta}$ reduces to the D.C. value. However, at a frequency of 10 kHz, in the case of a Mumetal lamination of 0.3 mm thick ($\mu_{rev} \approx 10^4 \cdot \mu_o$, $\rho \approx 0.6\ \mu\Omega$m) the values of the above coefficients are not negligible ($K_\theta \approx 4$; $\alpha \approx 1$). On the other hand, the presence of air-gaps, whose reluctance (high and constant) is in series with that of the core, makes variations in the reluctance of the core itself less important.

Analysis of ratio error by means of magnetic equations

As is well known, the magnetic structure of the C.T. can be represented schematically as in fig.7. The main magnetic circuit consists of two branches, each with an air-gap, designated respectively "i" and "e". The total leakage flux is represented by the flux path "d". The external primary winding carries the direct current I_{dc}, on which is superimposed a set of harmonics of which $\bar{I}_1$ denotes a generic one. The secondary winding, which is internal, being wound directly over the branch "i", has a resistance R_2 and is connected to the measuring resistance R_m. This winding carries the induced current $\bar{I}_2$ (harmonic corresponding to $\bar{I}_1$).

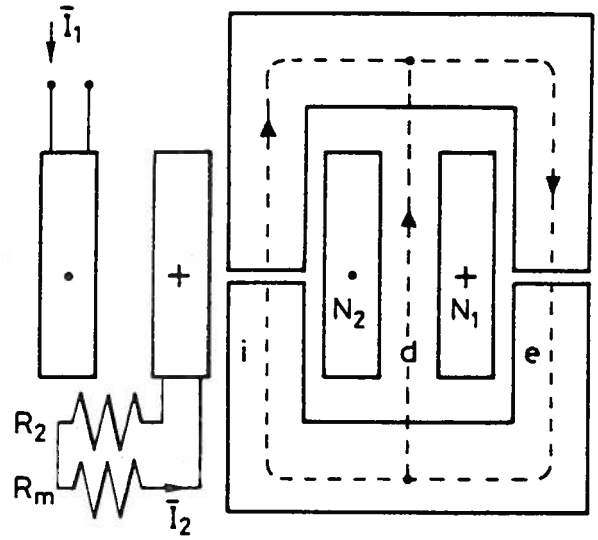

Fig.7. Schematic magnetic structure for the study of the current transformer.

As we have seen, the only effect of the direct current is to impose a value μ_{rev} to the permeability. This value, which is independent of the amplitude of the A.C. currents, affects both the core reluctance in the stationary condition and the values of the correction coefficients K_θ and α (via the penetration depth s_p).

The expressions for the reluctances in branches "i", "e" and "d" are as follows:

$$\bar{\theta}_i = \theta_g + \bar{\theta}_{fi} = \theta_g + \theta_{ofi} \cdot K_{\theta i} \cdot (1 + j \cdot \alpha_i)$$

$$\bar{\theta}_e = \theta_g + \bar{\theta}_{fe} = \theta_g + \theta_{ofe} \cdot K_{\theta e} \cdot (1 + j \cdot \alpha_e) \qquad (17)$$

$$\theta_d = \frac{1}{\mu_o} \cdot \frac{h_a}{p \cdot c'} \quad , \qquad c' = b + \frac{a_1 + a_2}{2} \quad ,$$

where "a_1", "a_2" and "b" are, respectively, the radial thicknesses of the primary and secondary windings, and the distance between these windings; "h_a" is the height of the windings, while "p" is their average circumference; θ_g is the reluctance associated to the geometrical air-gap.

On the basis of the directions of fluxes and currents shown in fig.7, the following magnetic equations can be written:

$$\begin{cases} \bar{\Phi}_i + \bar{\Phi}_d = \bar{\Phi}_e \\ N_2 \cdot \bar{I}_2 = \theta_d \cdot \bar{\Phi}_d - \bar{\theta}_i \cdot \bar{\Phi}_i \\ N_1 \cdot \bar{I}_1 = \theta_d \cdot \bar{\Phi}_d + \bar{\theta}_e \cdot \bar{\Phi}_e \end{cases} \quad (18)$$

Denoting with "ψ" the average flux linkages per turn, with "ψ_t" the total flux linkages of the windings and with "R_{2t}" the sum of the resistances R_2 and R_m, we can write:

$$\bar{I}_2 = \frac{\bar{E}_2}{R_{2t}} = \frac{j \cdot \omega \cdot \bar{\psi}_{2t}}{R_{2t}} \quad ; \quad (19)$$

The flux $\bar{\psi}_{2t}$ is expressed by:

$$\bar{\psi}_{2t} = N_2 \cdot (\bar{\psi}_i + \bar{\psi}_d) = N_2 \cdot (\bar{\Phi}_i + \sigma \cdot \bar{\Phi}_d) \quad , \quad (20)$$

where the coefficient σ acknowledges the fact that the average flux linkage per turn ψ_d (linked with the generic turn of the secondary winding) is a part of the flux $\bar{\Phi}_d$ of the leakage flux tube ($\sigma < 1$).

A precise calculation of the coefficient σ is difficult, as it depends on the division of the leakage flux between the primary and secondary windings. This division depends, amongst other factors, on the working conditions and on the saturation level of the magnetic circuit. In addition, the calculation of σ in any given situation would require a numerical resolution of the field.

Even in the past, this problem has been the subject of thorough studies [4]; an approximate estimate, which is useful in practice, of the coefficient σ can be made by attributing to the secondary winding all and only the leakage flux lines which go through the secondary itself in the axial direction. In this manner, putting F for the M.M.F. in the interspace between the windings (in fact, $F \approx F_1 \approx F_2$, having neglected the magnetizing M.M.F.), we have:

$$\sigma = \frac{\psi_d}{\bar{\Phi}_d} \approx \frac{\mu_0 \cdot \frac{p \cdot a_2/3}{h_a} \cdot F}{\mu_0 \cdot \frac{p \cdot c'}{h_a} \cdot F} = \frac{2 \cdot a_2}{3 \cdot (a_1 + a_2) + 6 \cdot b} \quad . \quad (21)$$

Inserting expressions (19) and (20) in eq.(18) and eliminating the fluxes, we arrive at the following expression for the ratio between the current phasors:

$$\frac{\bar{I}_2}{\bar{I}_1} = \frac{N_1}{N_2} \cdot \frac{\theta_d + \sigma \cdot \bar{\theta}_i}{\theta_d + (1 - \sigma) \cdot \bar{\theta}_e} \cdot \frac{1}{1 - j \cdot \frac{R_{2t}}{\omega \cdot N_2^2} \cdot \frac{\theta_d \cdot \bar{\theta}_i + \bar{\theta}_e \cdot \bar{\theta}_i + \theta_d \cdot \bar{\theta}_e}{\theta_d + (1 - \sigma) \cdot \bar{\theta}_e}} \quad . \quad (22)$$

On the other hand, we can assume:

$$\bar{\theta}_{fe} \approx \bar{\theta}_{fi} \approx \bar{\theta}_n/2 \quad , \quad (23)$$

where $\bar{\theta}_n$ represents the reluctance of the core, excluding the reluctances of the air-gaps: in fact, the two branches "i" and "e" have practically the same length and the same value of reversible permeability μ_{rev} (defined by the polarizing flux density B_{dc}).

On the basis of (23), eq.(22) approximates to the following:

$$\frac{\bar{I}_2}{\bar{I}_1} \approx \frac{N_1}{N_2} \cdot \frac{\theta_d + \sigma \cdot (\theta_g + \bar{\theta}_n/2)}{\theta_d + (1 - \sigma) \cdot (\theta_g + \bar{\theta}_n/2)} \cdot \frac{1}{1 - j \cdot \frac{R_{2t} \cdot (2 \cdot \theta_g + \bar{\theta}_n)}{\omega \cdot N_2^2}} \quad . \quad (24)$$

Substituting the expression for the core reluctance ($\bar{\theta}_n = \theta_{no} \cdot K_\varphi \cdot (1 + j \cdot \alpha)$), the ratio of the modulus values of the currents becomes:

$$\frac{I_2}{I_1} \approx \frac{N_1/N_2}{\sqrt{\left(1 + \frac{R_{2t} \cdot \theta_{no} \cdot K_\varphi \cdot \alpha}{\omega \cdot N_2^2}\right)^2 + \left(\frac{2 \cdot R_{2t}}{\omega \cdot N_2^2} \cdot (K_\varphi \cdot \theta_{no}/2 + \theta_g)\right)^2}} \cdot \sqrt{\frac{[\theta_d + \sigma \cdot (\theta_g + K_\varphi \cdot \theta_{no}/2)]^2 + (\sigma \cdot K_\varphi \cdot \alpha \cdot \theta_{no}/2)^2}{[\theta_d + (1-\sigma) \cdot (\theta_g + K_\varphi \cdot \theta_{no}/2)]^2 + [(1-\sigma) \cdot K_\varphi \cdot \alpha \cdot \theta_{no}/2]^2}} \quad ; \quad (25)$$

bearing in mind that, as the frequency increases, α tends to 1 while K_φ increases similarly to ξ, that is proportionally to $\sqrt{\omega}$, one can see that the first root in eq.(25) tends to unity. This confirms what can be deduced directly from analysis at low frequency:

$$\frac{I_2}{I_{1s}} \simeq \frac{1}{\sqrt{1 + \left(\frac{R_2 + R_m}{\omega \cdot L_0}\right)^2}} \quad ;$$

conversely, as the frequency increases, the second root in eq.(25) remains below unity, assuming a value which depends on the frequency and on the relative weighting of the reluctances involved.

Summarising, it can be concluded that the ratio of the currents is decreased by the presence of leakage fluxes and by eddy currents in the laminations.

The application of eq.(25) permits an evaluation of the ratio error, at least over the low-to-medium frequency range, up to the point where capacitance-type phenomena, due to capacitance between the turns, become noticeable.

Effects of the parasitic capacitances

Capacitance coupling between turns and between turns and earth have a considerable effect upon the functioning of the C.T.. This happens as soon as the respective impedances become comparable with those of the resistive and inductive types, which means above a certain frequency, whose value depends on the physical and construction parameters of the device.

In order to calculate the effects of capacitance, a model of reference [5], which employs a single lumped parameter, has been used. This model must be capable of reproducing the phenomena of major interest which can be observed when the device works in practice. In particular, it should show the first resonance peak of significant magnitude which can be seen of the amplitude/frequency response of the C.T., as the frequency increases.

The electrical equivalent circuit is shown in fig. 8.

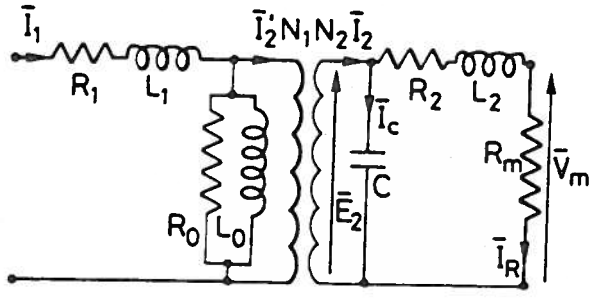

Fig.8. C.T. equivalent circuit adopted for the study of the effects of the parasitic capacitances.

All the capacitance effects are lumped into a single capacitor, pertaining to the secondary winding and situated after the ideal transformer.

On the basis of this circuit, it is useful to express the ratio between the currents in the following way:

$$\frac{\bar{I}_R}{\bar{I}_1} = \frac{\bar{I}_R}{\bar{I}_2} \cdot \frac{\bar{I}_2}{\bar{I}_1} \quad , \quad (26)$$

where $\bar{I}_R$ indicates the current flowing through the measuring resistance R_m, in this case different from the current $\bar{I}_2$.

As far as the ratio $\bar{I}_R/\bar{I}_2$ is concerned, its modulus is expressed by:

$$\frac{I_R}{I_2} = \frac{1}{\sqrt{(1-\omega^2 \cdot L_2 \cdot C)^2 + (\omega \cdot R_{2t} \cdot C)^2}} \quad ; \qquad (27)$$

The maximum value of this quantity, $(I_R/I_2)_{max}$, occurs at an angular frequency equal to:

$$\omega_{max} = \frac{1}{\sqrt{L_2 \cdot C}} \cdot \sqrt{1 - \frac{R_{2t}^2 \cdot C}{2 \cdot L_2}} \quad , \qquad (28)$$

Consequently, the value of $(I_R/I_2)_{max}$ is:

$$\left(\frac{I_R}{I_2} \right)_{max} = \frac{\sqrt{L_2/C}}{R_{2t}} \cdot \frac{1}{\sqrt{1 - \frac{R_{2t}^2 \cdot C}{4 \cdot L_2}}} \quad . \qquad (29)$$

On the other hand, the imaginary part of the impedance seen at the secondary terminals of the ideal transformer disappears (resonance condition) when the angular frequency is:

$$\omega_{res} = \frac{1}{\sqrt{L_2 \cdot C}} \cdot \sqrt{1 - \frac{R_{2t}^2 \cdot C}{L_2}} \quad ; \qquad (30)$$

At this frequency, the above current ratio becomes:

$$\left(\frac{I_R}{I_2} \right)_{res} = \frac{\sqrt{L_2/C}}{R_{2t}} \quad . \qquad (31)$$

On the basis of average numerical values of the parameters (see, for example, [6]), we have the following relations:

$$\sqrt{1 - \frac{R_{2t}^2 \cdot C}{L_2}} = 0.983 \ ,$$

and $\sqrt{1 - \frac{R_{2t}^2 \cdot C}{2 \cdot L_2}} = 0.992$; $\sqrt{1 - \frac{R_{2t}^2 \cdot C}{4 \cdot L_2}} = 0.996$;

because of this, it can be assumed that the resonance angular frequency (ω_{res}) and that corresponding to the maximum ratio (ω_{max}) are practically the same. This also applies to the following ratios:

$$\omega_{res} \approx \omega_{max} \approx \frac{1}{\sqrt{L_2 \cdot C}} \quad ;$$

$$\left(\frac{I_R}{I_2} \right)_{max} \approx \left(\frac{I_R}{I_2} \right)_{res} \approx \frac{\sqrt{L_2/C}}{R_{2t}} \quad . \qquad (32)$$

Finally, the total impedance as seen at the secondary terminals of the transformer in the resonance condition ($\omega = \omega_{res}$) is:

$$\bar{Z}_{2t(res)} = L/(R_{2t} \cdot C). \qquad (33)$$

As far as the ratio $\bar{I}_2/\bar{I}_1$ is concerned, as a first approximation one can assume that the expression (19) for the current $\bar{I}_2$ is modified as follows:

$$\bar{I}_2 = \frac{\bar{E}_2}{R_{2t}} + j \cdot \omega \cdot C \cdot \bar{E}_2 = \frac{\bar{E}_2}{[R_{2t}/(1 + j \cdot \omega \cdot R_{2t} \cdot C)]} \quad ; \qquad (34)$$

The comparison between equations (19) and (34) suggests that one can again refer to eq.(24), in order to substitute the quantity $R_{2t}/(1+j \cdot \omega \cdot R_{2t} \cdot C)$ for the total secondary resistance R_{2t}:

$$\frac{\bar{I}_2}{\bar{I}_1} \approx \frac{N_1}{N_2} \cdot \frac{\theta_d + \sigma \cdot (\theta_g + \bar{\theta}_n/2)}{\theta_d + (1 - \sigma) \cdot (\theta_g + \bar{\theta}_n/2)} \cdot \frac{1}{1 - j \cdot \frac{R_{2t} \cdot (2 \cdot \theta_g + \bar{\theta}_n)}{(1 + j \cdot \omega \cdot R_{2t} \cdot C) \cdot \omega \cdot N_2^2}} \quad . \qquad (35)$$

The quantitative analysis of eq.(35) allows to retain as still valid the remarks made in connection with eqs.(24) and (25), in that the capacitance appears in the denominator only, the modulus of which tends to unity also in this case. In addition, the similarity of behaviour between equations (35) and (24) is also quantitative in nature, considering that the correction term $(\omega \cdot R_{2t} \cdot C)$ is rather small compared of frequencies being considered (f < 10 kHz).

Summarising, it can be concluded that, for the purpose of determining the ratio $\bar{I}_R/\bar{I}_1$, the term of major importance is the ratio $\bar{I}_R/\bar{I}_2$, while the term $\bar{I}_2/\bar{I}_1$ is, in practice, almost the same as that obtained from magnetic equations only.

CONCLUSIONS

The present work consisted of a study of design methods and the analysis of performance of a current transformer subjected to a D.C. bias. The considered C.T. is a device for the detection of the harmonic content produced on the D.C. side of a static convertor. The frequency range of interest is $10 \div 10^4$ Hz and the amplitude of the A.C. components is of the order of $10^{-3} \div 10^{-4}$ times the D.C. component.

On the basis of a simplified model, valid at low frequencies, an algorithm has been developed for the design of the device, starting from nominal and design quantities expressed either in specific or non-dimensional form.

A more complete model of the C.T. has then been developed, capable of evaluating the ratio error over the entire frequency range of interest. The model takes into account leakage fluxes, the loss and reactive effects of eddy currents in the magnetic material and the effect of the equivalent capacitance of the windings.

These studies have led to the contruction of a C.T. prototype. The results of experimental tests on the device and of simulaton studies based on the mathematical model will form the subject of a further detailed study [6].

REFERENCES

[1] A. Di Gerlando, I. Vistoli: "Special Transformers for the Measurement of Harmonic Noise of D.C. Currents"; Symposium "SPEEDAM", 19-21 May 1992, Positano, Italy.

[2] R. Bozorth: "Ferromagnetism"; D. Van Nostrand, New York, 1951.

[3] P. Bunet: "Courants de Foucault"; Librairie J. B. Baillière et fils, Paris, 1933.

[4] F. Correggiari: "Sulla scissione della reattanza di corto circuito dei trasformatori"; L'Elettrotecnica, Vol. XLI, N°1, Genuary 1954, page 2.

[5] D. A. Douglass: "Current Transformer Accuracy with asymmetric and high Frequency fault Currents"; IEEE Trans. on P.A.S., Vol. PAS-100, N°3, March 1981.

[6] A. Di Gerlando, I. Vistoli: "D.C. polarized Current Transformers for the Measurement of Harmonic Noise: Numerical and experimental Analysis"; ICHPS V Conference, Atlanta, Georgia, USA, September 23-25, 1992.

[7] I. Johansen: "Natural Frequencies in Power Transformer Winding"; Trans. of AIEE, Vol. PAS-78, Part IIIA, June 1959, page 129.

[8] R. C. Degeneff: "A general method for determining resonance in trasformer windings"; IEEE Trans. on P.A.S., Vol. PAS-96, N°2, 1977.